

# ACOUSTIC DETECTION AND LOCALIZATION OF WHALES IN BAY OF FUNDY AND ST. LAWRENCE ESTUARY CRITICAL HABITATS

Yvan Simard<sup>1,2</sup>, Mohammed Bahoura<sup>3</sup> and Nathalie Roy<sup>2</sup>

<sup>1</sup>ISMER, Université du Québec à Rimouski, P.O. Box 3300, Rimouski, Québec, Canada G5L 3A1

<sup>2</sup>Maurice Lamontagne Institute, Fisheries & Oceans Canada, P.O. Box 1000, Mont-Joli, Québec, Canada G5H 3Z4

<sup>3</sup>Département de Mathématiques, Informatique et Génie, Université du Québec à Rimouski,  
P.O. Box 3300, Rimouski, Québec, Canada G5L 3A1

## ABSTRACT

The detection and localization of marine mammals using passive acoustics is explored for two critical habitats in Eastern Canada. Two-dimensional hyperbolic localization is performed on time differences of arrivals of specific calls on grids of coarsely spaced autonomous recorders and on a shore-linked coastal array of closely spaced hydrophones. Delays are computed from cross-correlation and spectrogram cross-coincidence on signals enhanced with high-frequency emphasis and noise spectral suppression techniques. The outcomes and relative performance of the two delay estimation methods are compared. The difficulties encountered under the particular conditions of these two environments are discussed for the point of view of automated localisation for monitoring whales.

## RÉSUMÉ

La détection et la localisation de mammifères marins à l'aide de l'acoustique passive est explorée pour deux habitats critiques dans l'est du Canada. La technique de localisation par hyperboles en deux dimensions est utilisée à partir des différences de temps d'arrivée à des réseaux de systèmes d'enregistrements autonomes largement espacés, ainsi qu'à un réseau serré d'hydrophones reliés à la côte. Les délais d'arrivée sont calculés par inter-corrélation ainsi que par inter-coïncidence des spectrogrammes des signaux rehaussés par des techniques de rehaussement des hautes fréquences et de soustraction spectrale du bruit. Les résultats et la performance relative des deux méthodes sont comparés. Les difficultés rencontrées dans le contexte des conditions particulières de ces deux environnements sont discutées par rapport à l'automatisation de la localisation pour le monitoring des baleines.

## 1. INTRODUCTION

The localisation of living sound sources in the marine environment from the time difference of arrivals (TDoAs) at a series of receivers is several decades old (Watkins and Schevill 1972, Cummings and Holliday 1985). The most common localization method from large aperture arrays is hyperbolic fixing (Spiesberger and Fristrup 1990, Spiesberger 1999, 2001), though other simple (Cato 1998) or more elaborated model-based methods could be used (e.g. Tiemann and Porter 2003). With the fast development of electronic and computer technology, the setting up of such passive acoustic systems for non-intrusively monitoring whales in their environment is becoming increasingly available and spreading rapidly. This approach proved useful to gather information on the annual migrations of baleen whales over large oceanic basins (e.g.

Watkins et al. 2000). It is now sought for monitoring time-space use of habitat in intensively frequented meso-scale hot spots, eventually in real time, with the aim of improving their protection. Population density indices can also be estimated from such listening arrays (McDonald and Fox 1999), and used to follow its growth or displacement. Though the theory is well documented, its application in the field must be tuned to the particular characteristics of the local environment. This is especially important for implementing automated detection and localization algorithms. This paper is a preliminary exploration of the performance of simple techniques adapted to the conditions encountered in two critical habitats intensively visited by several species of whales during summer in eastern Canada, the Bay of Fundy and the Saguenay—St. Lawrence Marine Park.

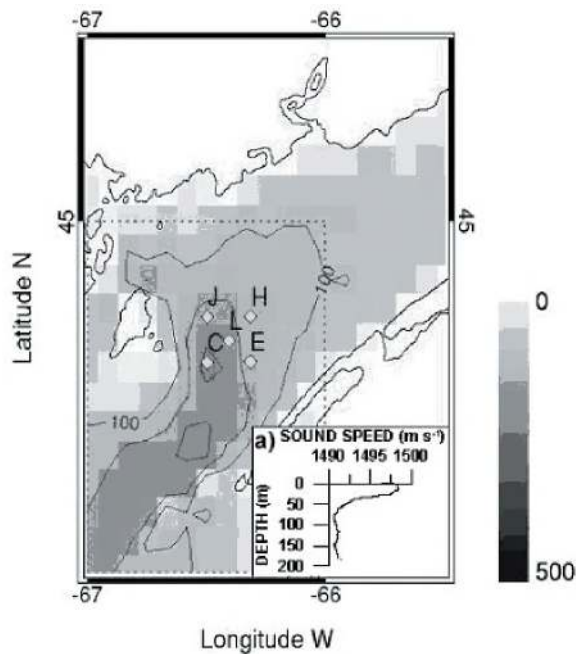


Figure 1. Bay of Fundy study area, with the bathymetry, the location of the 5 OBHs, and a typical sound speed profile.

## 2. MATERIAL AND METHODS

### Data collection

The Bay of Fundy data set was collected in September 2002, with 5 ocean bottom hydrophones (OBHs), deployed in a centred square configuration with sides of 14.26 km, at

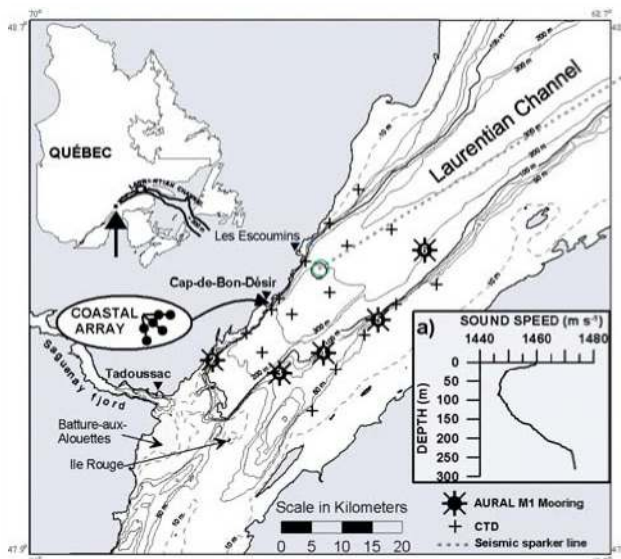


Figure 2. Study area in Saguenay—St. Lawrence Marine Park, with bathymetry, locations of the 6-hydrophone coastal array and the 5 AURAL M1 autonomous hydrophones, CTD stations and the track of a seismic-sparker RV (dotted line), with a typical sound speed profile.

the head of the ~200 m deep channel (Fig. 1). The OBH depths varied from 123 m to 210 m. The omnidirectional hydrophones (OAS model E-2SD, flat receiving sensitivity (RS) from 50 to 700 Hz) were 0.9 m from the bottom. The OBH positions were cross checked by interrogating their acoustic pinger and were accurate to 2 to 13 m. The clock drift over the 9-day deployment was negligible (<1 ms to 34 ms). The data were digitized with a 12-bit A/D converter sampling the 800 Hz low-pass signal at 1200 Hz. The OBH J RS was ~20 dB lower than the others. Temperature (XBTs) and conductivity (CTD) profiles (e.g. Fig. 1a) were performed during the experiment. A second data set was collected in August 2000 with 4 OBHs and a sampling frequency of 5000 Hz. A "calibration signal" representing right whale calls was then transmitted (source level of 155-160 dB re 1  $\mu$ Pa) from a rhib boat.

The St. Lawrence data sets were collected in August-September 2003 on the whale feeding ground at the head of the Laurentian channel (c.f. Simard et al. 2002), with a 6-hydrophone coastal array and a series of 5 autonomous hydrophones (AURAL M1, Multi-Electronics, Rimouski, QC, Canada) (Fig. 2). All hydrophones were omnidirectional HTI 96 MIN (flat RS from ~4 Hz to 30 kHz). The coastal array (Fig. 2) was deployed along Cap-de-Bon-Désir with three 600-m cables, each with 2 hydrophones, plunging into the sound channel (Fig. 2a). These hydrophones were ~5 m above the bottom. The array aperture was 657 m. The data were acquired without

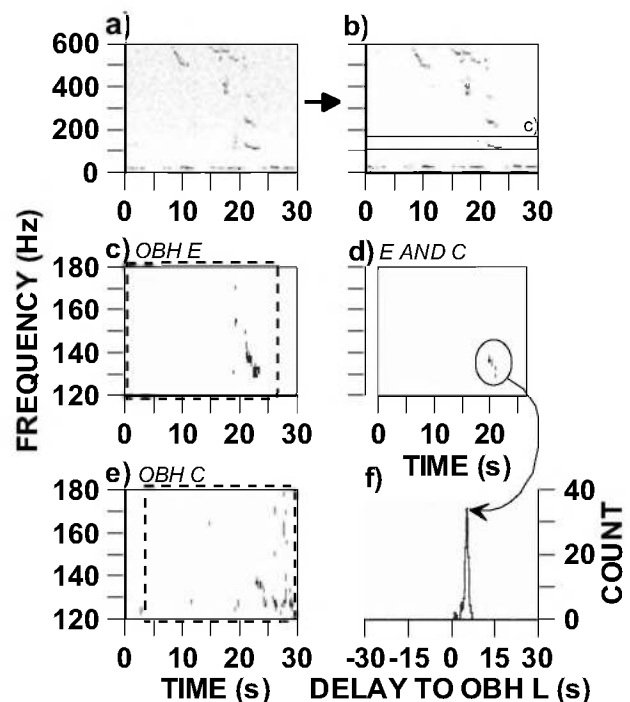


Figure 3. Example of computation of TDoA from spectrogram image cross-coincidence for Bay of Fundy low-frequency call S131-13 (see text).

interruption with fully-synchronous 16-bit A/Ds and DSPs mounted on a ChicoPlus data acquisition card (Innovative Integration, Ca, USA), sampling at 20 kHz. The exact hydrophone positions were determined from acoustic pulses transmitted from the R/V Coriolis II at a grid of stations off the array, where CTD profiles were also made

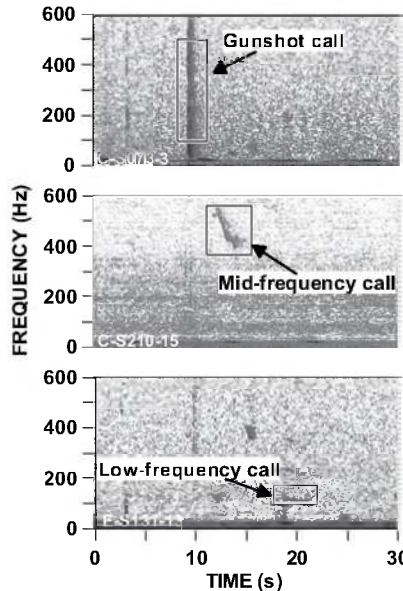


Figure 4. Spectrograms of OBH records showing the three types of northern right whale calls looked for in the Bay of Fundy data set.

for sound speed measurements. The AURAL M1 autonomous hydrophones were deployed in the sound channel (~50-60 m) on standard oceanographic moorings using sub-surface buoys. They were deployed 8-14 km apart along the border of the channel, in an arc facing the coastal array. Their position, as determined with DGPS, was precise to better than ~10 m, from crosschecks of the mooring echoes on the R/V scientific echosounders. The AURALS M1 record the depth and the ambient temperature besides the acoustic data. These 16-bit acoustic data were acquired at the 2000 Hz optional sampling rate of the AURALS M1, which includes a corresponding anti-aliasing (low-pass) filter. The internal clocks were synchronised to the microsecond with the PPS (pulse per second) signal of the GPS at the start of the recordings. The relative clock drifts were measured by synchronising all units at the recovery on a simultaneously recorded sound. CTD profiles were made at a grid of stations covering the study area at the beginning and the end of the recording period (Fig. 2).

#### Data analysis

The localization process from the TDoAs at the hydrophones proceeded in three steps. First, the frequency band of the selected whale call or anthropogenic sound was determined by visual inspection of the spectrogram (e.g. Fig. 3). Second, the signal was conditioned for TDoA finding algorithms, by high frequency pre-emphasis and noise spectral subtraction (Martin 2001) as follows (c.f. Fig. 4).

Pre-emphasis filter:

$$y_p(i) = y(i) - a y(i-1), \quad \text{where } 0.96 < a < 0.99 \quad (1)$$

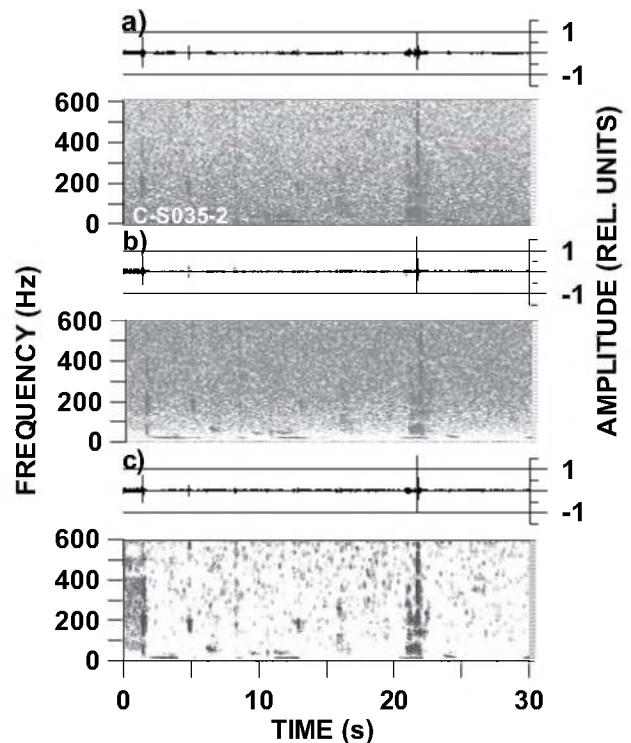
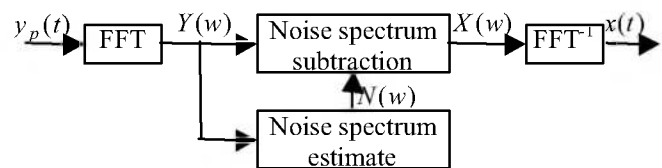


Figure 5. Waveforms and spectrograms of an OBH record containing a gunshot call, raw (a), after high-frequency pre-emphasis (b) followed by noise spectral subtraction (c).

Noise suppression:

$$y_p(t) = n(t) + x(t) \quad (2)$$



where  $Y(w)$  and  $N(w)$  are smoothed over window lengths chosen to maximize the difference between  $x(t)$  and  $n(t)$ .

Third, the TDoAs between the hydrophones were computed on the waveform using cross-correlation. Data were first normalised to a 0-1 scale and then filtered (4<sup>th</sup> order high-pass or band-pass Butterworth) to keep only data in the selected call band. The absolute value of the cross-correlation series was low-pass filtered (2<sup>nd</sup> order Butterworth) to remove spikes hindering precise TDoA detection close to the maximum. The TDoAs were also computed from spectrogram "cross-coincidence" (Tiemann et al. 2001). The spectrogram of  $y_p(t)$  or  $x(t)$  is transformed to a binary image using a threshold value corresponding to the 95<sup>th</sup> or 99<sup>th</sup> percentile of the cumulative frequency distribution (cfd) of the spectrum values (Fig. 3a-b). The spectrograms are computed with a FFT window of 256 or

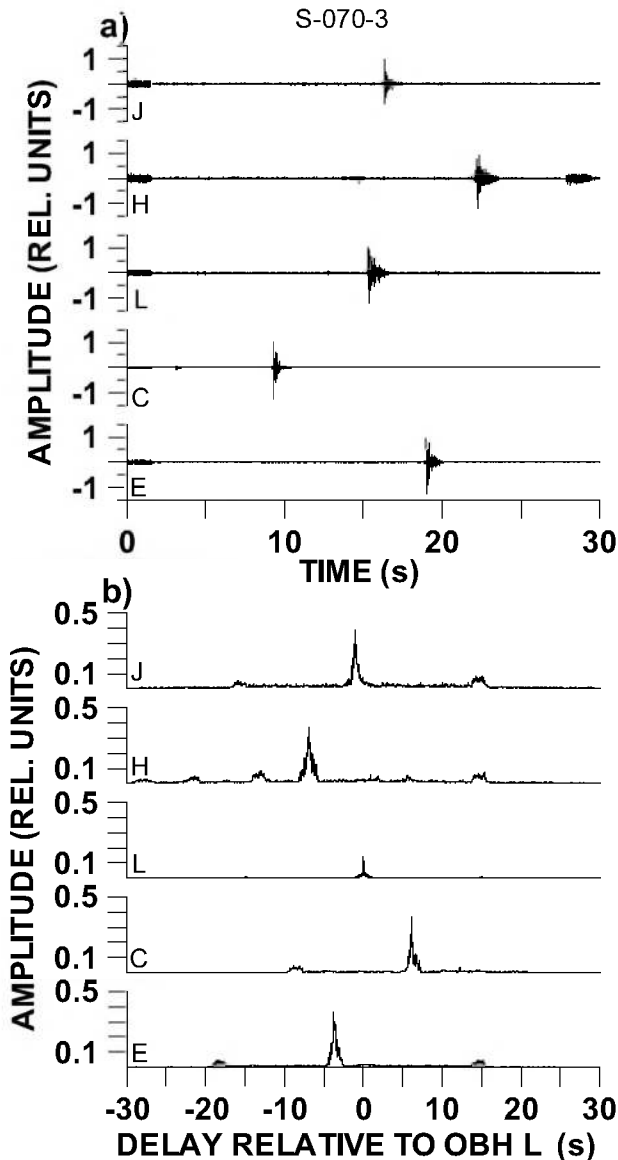


Figure 6. Conditioned and filtered OBH records (a) with their corresponding filtered cross-correlation series (b), for one gunshot call in the Bay of Fundy.

512 points, with 60% overlap. The frequency band of interest is extracted (Fig. 3c and e), and a logical *AND* is computed between the binary images of the hydrophone pair, for each time lag (Fig. 3c and e boxes). The resulting image for a given lag (Fig. 3d) has pixel values of 1 only when two positive pixels coincide on both images. The sum of these pixels represents the level of coincidence between the two spectrograms for the corresponding lag. A cross-coincidence series is obtained by expanding to all lags (Fig. 3f) for TDoA detection.

A constant sound speed of 1491 m/s, corresponding to the lower part (>50 m) of the water column (Fig. 1a), was used for the Bay of Fundy. For the St. Lawrence, it was

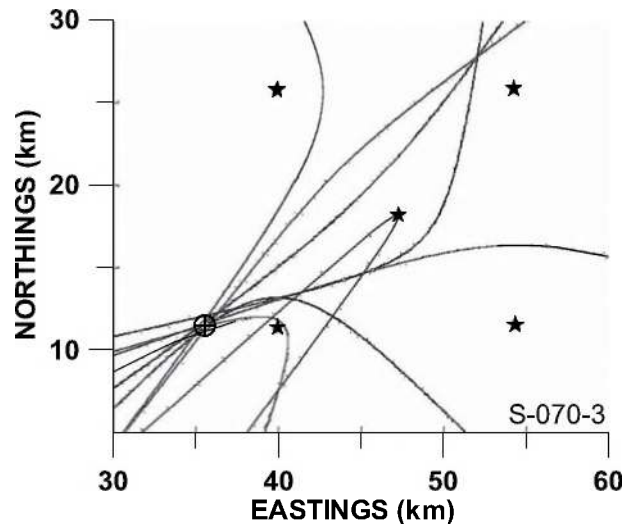


Figure 7. 2D hyperbolic localization of the gunshot call from Fig. 5 TDoAs. Position is: 44.6028° N, 66.5522° W. Rms error of the fixing was 197 m.

1450 m/s, which is the average speed in the sound channel where the hydrophones were deployed (Fig. 2a). Coordinates were transformed to (and from) Cartesian units using a Lambert projection. The 2D hyperbolic localization used the *LocateDelays.m* Matlab script (Dave Mellinger web site). This algorithm rejects delays that are larger than the maximum travel time between the hydrophone pairs given the constant sound speed. TDoAs that do not fit to this model are thus ignored for hyperbolic fixing. The predicted  $TDoA_c$  from the travel time differences between the estimated source location and the hydrophones are computed for the  $n$  valid hydrophone pairs, and the rms error relative to the observed  $TDoA_o$  is estimated as follows:

$$\sqrt{\sum_n (TDoA_o - TDoA_c)^2 / n - 2} \quad (3)$$

The hyperbolic fixing uncertainty is obtained by converting this time error into distance error by multiplying by the sound speed.

### 3. RESULTS

The Bay of Fundy test data files provided for the workshop were separated into three types of North Atlantic right whale calls: gunshots, low-frequency and mid-frequency calls (Fig. 4). The selected frequency bands for these calls were respectively: 100 to 500 Hz, 100 to 180 Hz and 350 to 500 Hz for cross-coincidence, and 50 to 600 Hz, 100 to 300 Hz, and 400 to 600 Hz for cross-correlation. An example of the pre-conditioning of the signal is shown in Fig. 5. The TDoA estimation from cross-correlation is depicted in Fig. 6 for one gunshot sound. Resulting 2D hyperbolic fixing for that sound is shown in Fig. 7.

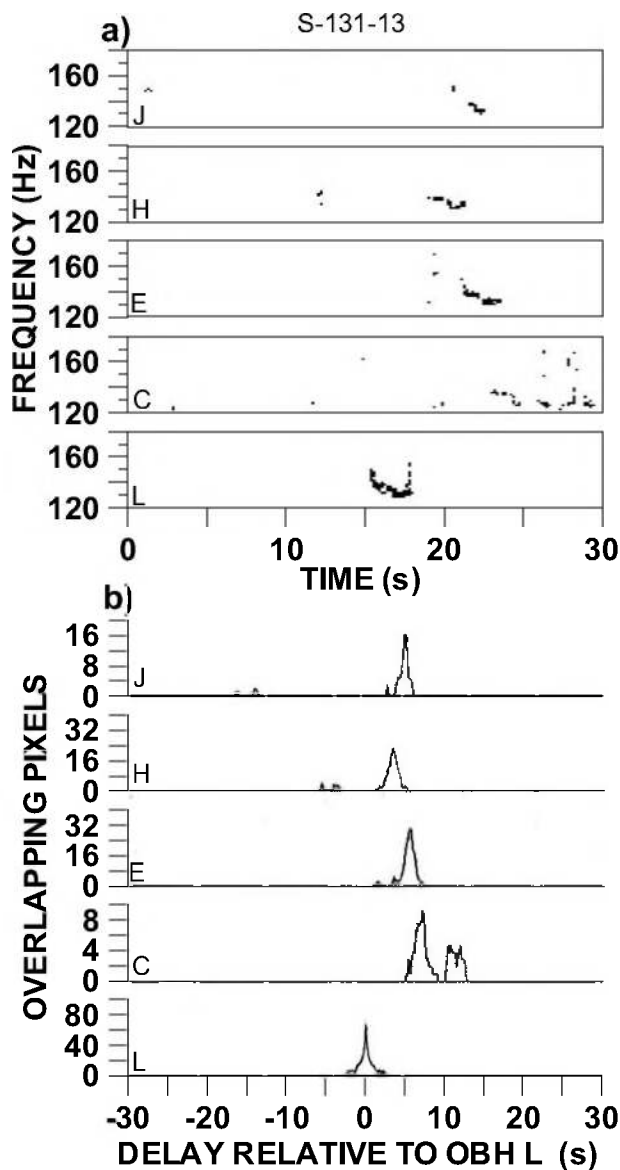


Figure 8. Binary images of the spectrograms of S-131-13 low-frequency call in Bay of Fundy for the five OBHs (a), and the corresponding cross-coincidence relative to OBH L (b).

TDoAs estimation with  $y_p(t)$  spectrogram cross-coincidence is shown in Fig. 8 for a North Atlantic right whale low-frequency call recorded in Bay of Fundy. The localisation of the call is presented in Fig. 9. For the 15 North Atlantic right whale calls of the Bay of Fundy data set, the two TDoA estimation methods generally produced similar hyperbolic fixings (Fig. 10-11, Table 1). The differences between the two methods is generally less than 450 m, except for the distant mid-frequency calls, located more than 25 km from the nearest OBH (Table 1, Fig. 11). However, the fixing error (Table 1, Fig. 10) showed that the spectrogram cross-coincidence method had difficulties with

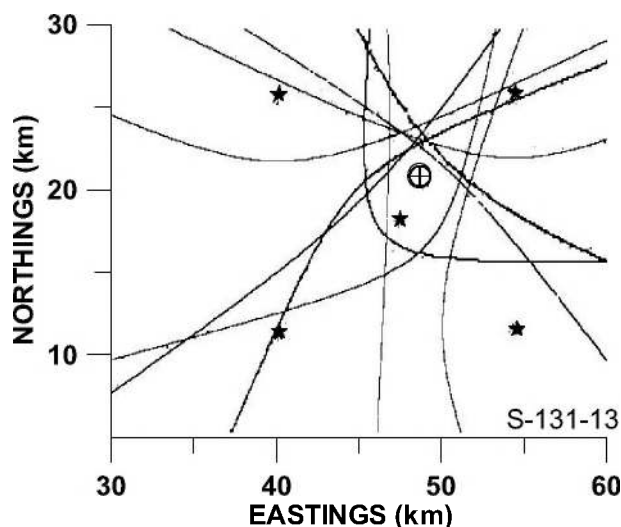


Figure 9. 2D hyperbolic localization of the low-frequency call from Fig. 8 TDoAs. Position is: 44.6856° N, 66.3879° W. Rms error of the fixing was 381 m.

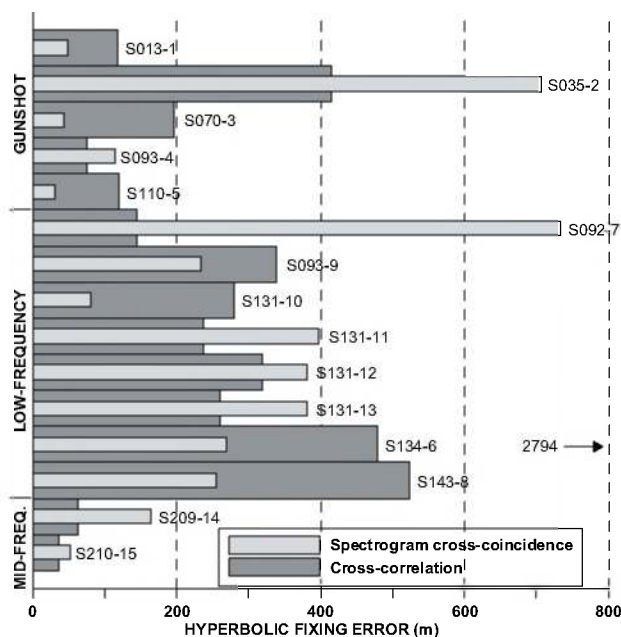


Figure 10. Comparison of hyperbolic fixing rms error obtained with the two TDoA estimation methods for Bay of Fundy call data set. Crosscorrelation for call S134-6 was done on  $y_p(t)$  instead of  $x(t)$ , the latter producing an error of 2794 m.

two calls and the cross correlation method with one call (see Discussion).

The binary images of the  $x(t)$  spectrograms of a 30-s long low frequency beluga phrase, detected on the 5 AURAL M1 moorings in the St. Lawrence, is presented in

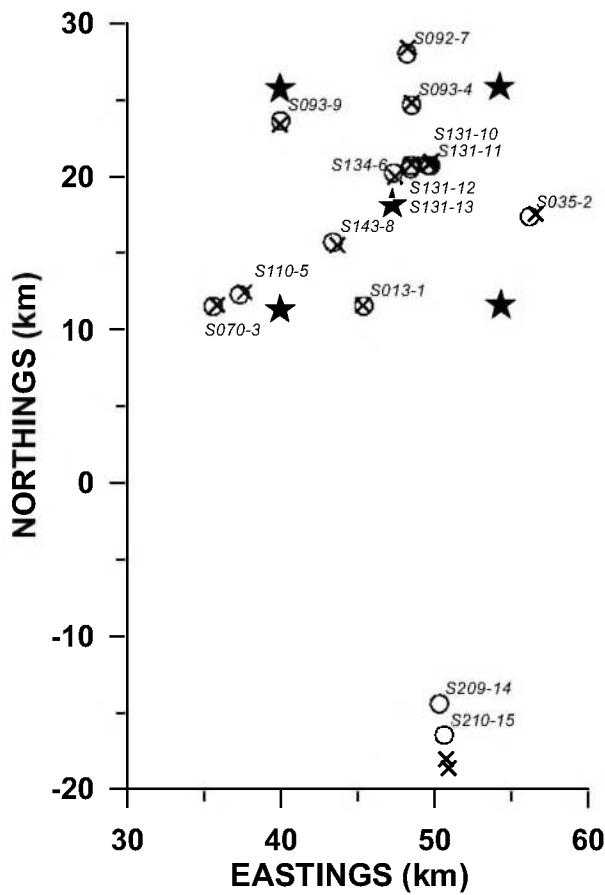


Figure 11. Localization of the 15 northern right whale calls of the Bay of Fundy data set, for TDoAs from spectrogram cross-coincidence (×) and cross-correlation (○), with the positions of the OBHs (★).

Fig. 12a. Its intensity is much higher on instruments #3 and #4. The record from instrument #2 has additional strong vocalisations, likely from close-by minke whales (Fig. 12a, dashed-line box). In computing the TDoAs for this call using spectrogram cross-coincidence, these minke whale calls had to be masked to get the right TDoA for the instrument #2, so that it corresponds to the TDoA estimate from manually inspecting the spectrograms. The localisation obtained that way is presented in Fig. 13. The one from the TDoAs obtained by manually inspecting the spectrograms differs from only 159 m from that position. The hyperbolic fixing rms error was large (2.5 km) in both cases. Figure 14a illustrates another example of a cluck clearly recorded on the AURAL M1 moorings, except for the instrument # 5 where it was severely masked by flow noise. The TDoAs estimated from cross-correlation of the  $y_p(t)$  series were the same as those obtained from manually inspecting the spectrograms. The hyperbolic fixing used only a few of them though (Fig. 14b), the other ones were exceeding the expected maximum delays from the assumed sound speed

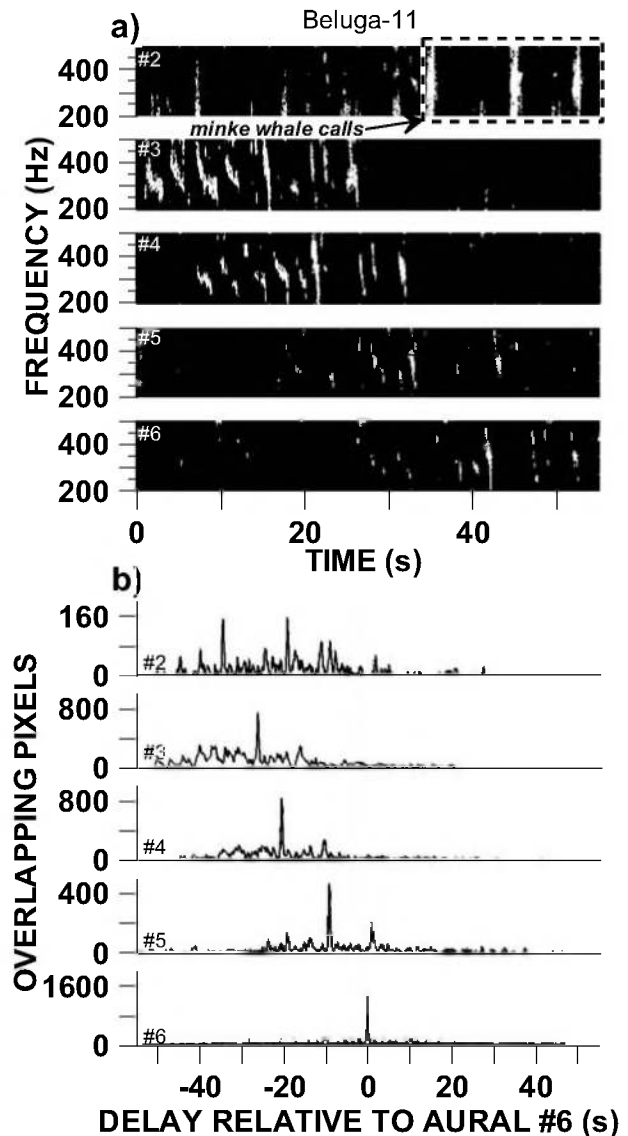


Figure 12. Binary images of the spectrograms of a beluga low-frequency call phrase from the St. Lawrence Estuary five AURALS M1 moorings (a), and the corresponding cross-coincidence (b). The minke whale calls (dashed line box) were removed for computing the AURAL M1 #2 cross-coincidence series.

and declared invalid. The pings of a towed seismic sparker echosounder were used to localise a R/V working in the area from the AURAL M1 recordings (Fig. 2). All methods failed to find the TDoAs. A closer look at the spectrograms showed that some pings at the start of the sounding line were missing on two instruments in the narrow bandwidth (1 kHz) of the observations (source peak was  $\sim 2.2$  kHz from the coastal array). When corrected for these missing pings, the TDoAs obtained by manually inspecting the spectrograms successfully localised the R/V at the start of its sounding line (Fig. 2, circles). The error with the true DGPS position of the 50-m R/V was 233 m, which is very

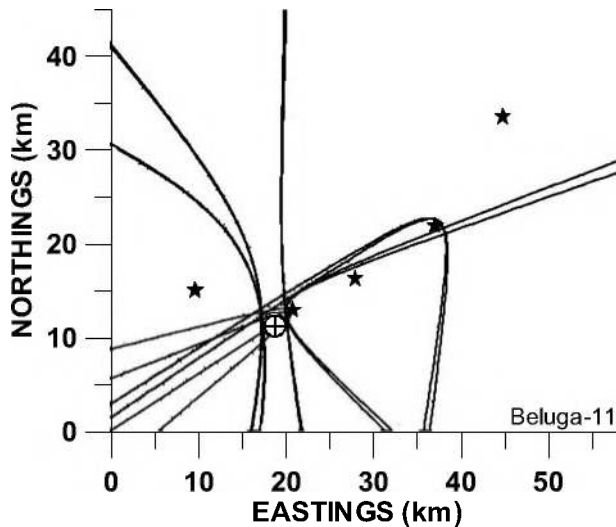


Figure 13. 2D hyperbolic localization of the low-frequency beluga call from Fig. 12 TDoAs. Position is: 48.1553° N, 69.4697° W.

small given that the distance between the DGPS antenna and the towed sparker was larger than 70 m.

A 1600-2600 Hz beluga whistle (Figs.15) from the 6-hydrophone coastal array was localized using TDoAs from spectrogram cross-coincidence. It was recorded 12 min before the beluga-11 call (Figs. 12-13) and localised in the same part of the observed area, 5 km off the array and 7.8

km away from the beluga-11 call (Fig. 16).

#### 4. DISCUSSION

This exercise of localizing whale calls using passive acoustics in two critical habitats in eastern Canada gives an example of the performance of simple techniques in actual conditions at sea. The accuracy of source localization depends on precision of measurements of TDoAs, hydrophone positions, sound velocity and the geometry of the hydrophone network (Wahlberg et al. 2001). Precise estimation of TDoAs is critical for accurate localization. This relies on both the acquisition and the processing of the data. Substantial effort has been dedicated to precise 3D localization of the hydrophones and accurate synchronization of all recording clocks in both study areas. Though the error due to the equipment may be minimized, it is not zero because of the difficulty of accurate x y z positioning of the receivers at sea, fluctuating sound speed structures and water depth with tides, and tilting of the mooring line or displacement of bottom mounted instruments with strong currents. The level of precision required for the 3D position of the hydrophones is particularly high for the coastal array, because of the close spacing of the hydrophones and the very small TDoAs of the calls.

Table 1. 2D hyperbolic localization of Bay of Fundy northern right whale calls using TDoAs computed with spectrogram cross coincidence and cross-correlation.

File	Type	Spectrogram cross-coincidence						Cross-correlation					
		Band (Hz)	FFT (pt)	Cfd cut-off	Lat. N	Long. W	error (m)	error (m)	Lat. N	Long. W	Band (Hz)	X-correlation Low-pass filter cut-off (Hz)	Localization differences (m)
S013-1	Gunshot	100-500	256	0.99	44.6027°	66.4289°	49	118	44.6025°	66.4284°	50 - 600	36	45
S035-2	Gunshot	100-500	256	0.99	44.6559°	66.2865°	707	415	44.6541°	66.2916°	50 - 600	36	451
S070-3	Gunshot	100-500	256	0.99	44.6036°	66.5493°	42	197	44.6028°	66.5522°	50 - 600	36	247
S093-4	Gunshot	100-500	256	0.95 <sup>1</sup>	44.7216°	66.3876°	115	75	44.7203°	66.3880°	50 - 600	36	148
S110-5	Gunshot	100-500	256	0.95 <sup>2</sup>	44.6112°	66.5264°	30	120	44.6096°	66.5303°	50 - 600	36	357
S092-7	Low-frequency call	100-180	512	0.99	44.7538°	66.3908°	734	144	44.7506°	66.3914°	100 - 300	12	359
S093-9	Low-frequency call	100-180	512	0.99	44.7095°	66.4969°	234	339	44.7117°	66.4958°	100 - 300	12	260
S131-10	Low-frequency call	100-180	512	0.99	44.6858°	66.3741°	80	279	44.6850°	66.3753°	100 - 300	12	130
S131-11	Low-frequency call	100-180	512	0.99	44.6867°	66.3728°	397	237	44.6846°	66.3727°	100 - 300	12	233
S131-12	Low-frequency call	100-180	512	0.99	44.6856°	66.3879°	381	319	44.6850°	66.3887°	100 - 300	12	92
S131-13	Low-frequency call	100-180	512	0.99	44.6856°	66.3879°	381	260	44.6831°	66.3891°	100 - 300	12	294
S134-6	Low-frequency call	100-180	512	0.99	44.6785°	66.4017°	269	479 <sup>3</sup>	44.6806°	66.4032°	100 - 300	12	262
S143-8	Low-frequency call	100-180	512	0.99	44.6382°	66.4503°	255	523	44.6402°	66.4534°	100 - 300	12	331
S209-14	Mid-frequency call	350-500	512	0.99	44.3357°	66.3641°	164	62	44.3684°	66.3688°	400 - 600	6	3653
S210-15	Mid-frequency call	350-500	512	0.99	44.3303°	66.3619°	53	37	44.3500°	66.3650°	400 - 600	6	2203
S282	Calibration call	420-480	512	0.99	44.6945°	66.3801°	430						
S288	Calibration call	525-580	512	0.99	44.6945°	66.3802°	271						
S289	Calibration call	525-580	512	0.99	44.6943°	66.3807°	354						

<sup>1</sup> Failed with a cut-off of 0.99; <sup>2</sup> Less precise with a cut-off of 0.99; <sup>3</sup> Without noise spectral subtraction.

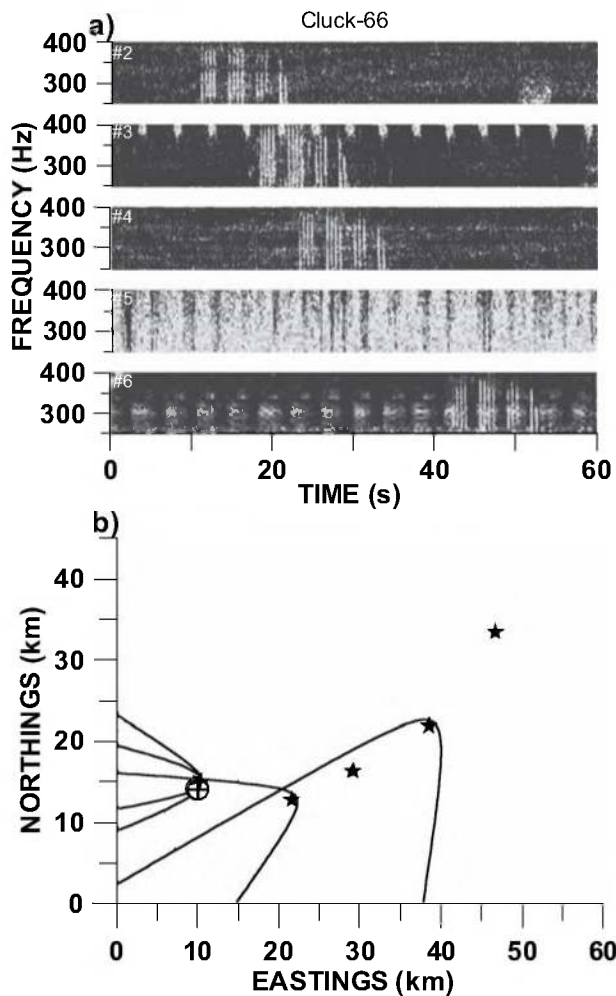


Figure 14. Spectrogram of cluck for the 5 AURAL M1 moorings in the St. Lawrence (a) and its hyperbolic fixing using TDoAs from cross-correlation (b).

Precise TDoAs also relies on signal strength relative to noise (SNR) at each hydrophone of the localization network. The three data sets showed that this is very variable and not only depends on propagation effects and travel distances, but also on masking noise (from shipping, flow, etc.). The low sensitivity of OBH J was however involved in some cases. The conditioning of the data for optimal TDoA detection helped to cancel out some of these effects. The two signal-processing steps we used to increase the SNR before computing the TDoAs proved useful to handle most calls with the same algorithm. Exceptions were encountered where the noise spectral suppression also removed the faint signals (e.g. cluck call of Fig. 14, and S134-6 call, Table 1). A step should therefore be added here to decide when noise suppression should be employed, and which parameters are best suited to the type of call considered. The spectrogram cross-coincidence method required noise spectral suppression only in very low SNR conditions, such as when shipping noise was high at some hydrophones, which was

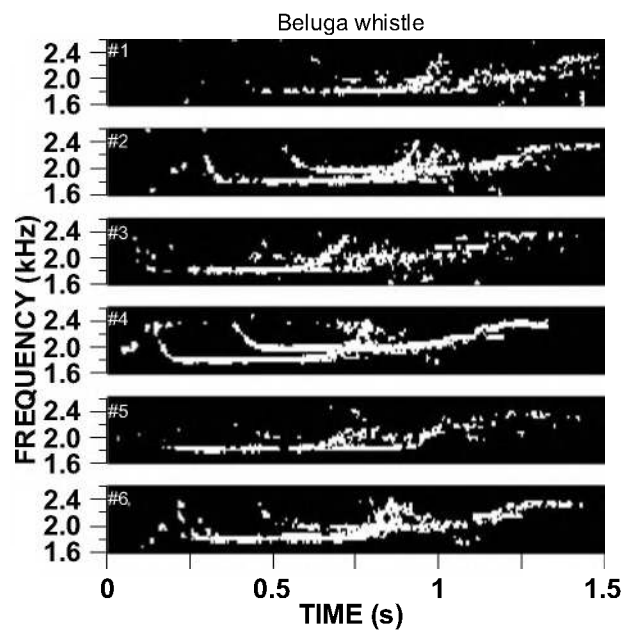


Figure 15. Binary images of the spectrograms of a beluga whistle from the St. Lawrence Estuary 6-hydrophone coastal array.

the case for the beluga call of Fig. 12. For the transformation of the spectrogram into a binary image, low SNR sometimes forced the lowering the cumulative frequency distribution cutoff from 0.99 to 0.95 (e.g. gunshot calls S093-4 and S110-5 of Table 1). Very low SNRs for OBH J and C are at the origin of the two large fixing errors for calls S035-2 and S092-7 with the spectrogram cross-coincidence method (Table 1). In this case, it would be better to drop the low SNR OBH and perform the hyperbolic fixing with only four instruments. For an unsupervised automatic fixing algorithm, another decision step should be added to reject too low SNR recordings. The filtration of the series, to remove the spikes that often occur close to the maxima before the peak detection, also appeared necessary for more

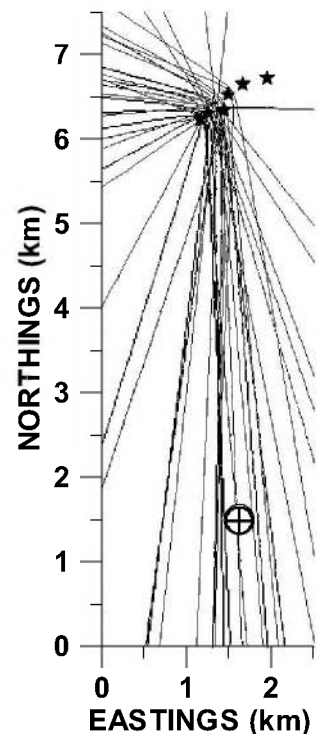


Figure 16. Hyperbolic fixing of the beluga call of Fig. 15 using TDoAs from spectrogram cross-coincidence.



robust TDoA detection with the cross-correlation method. A supervised decision was necessary to get the TDoA for the beluga call on the AURAL M1 #2 when close minke whale calls prevented its accurate estimation. This is likely to occur in critical habitats that are frequented by several whales, such as the Saguenay—St. Lawrence Marine Park. The masking of concurrent calls is then necessary and could be accomplished by connecting the TDoA finding algorithm with the prior step of call detection and classification.

The geometry of the hydrophone network is of course another important aspect affecting the precision of the localization. The centered square configuration of the Bay of Fundy OBHs, with a relatively small total width (14.26 km) insured close enough spacing (10.36 km) between all hydrophones to receive the call with a good SNR on all instruments in most cases. The arc shape of the St. Lawrence AURAL M1 configuration (which resulted from the loss of one instrument in a planned U-configuration) is less effective because of the solution for the left-right ambiguity is dependent on a single instrument, and because of the large distances (> 20 km) between the distant hydrophones. Propagation effects then become important, and the conditions are far from the linearity assumption of hyperbolic fixing (Spiesberger and Wahlberg 2002). The arrival times were increasingly late, as a function of the travel time, compared to the assumed direct path at a constant sound speed. The vertical sound speed gradient in the St. Lawrence is about three times larger than in the Bay of Fundy (c.f. Figs. 1a and 2a). This resulted in the dropping of those TDoAs exceeding the expected maximum delays between the instruments, and the localization with only a few instruments (e.g. Fig. 14). The sound speed should be allowed to change with travel time, as proposed by Spiesberger and Wahlberg (2002). A multipath propagation model (e.g. Tiemann et al. 2001) should therefore be used for proper source localization for ranges larger than the few kilometers where the direct path assumption is valid in these shallow environments. Another relevant aspect of receiver geometry is the vertical localization of the hydrophone. The Bay of Fundy and the St. Lawrence coastal array hydrophones were placed close to the bottom and therefore subject to shadow zones and interference with bottom reflections. These latter were likely contributing to errors in TDoA detection. For the St. Lawrence coastal array, the delay error could be proportionally large because of the close spacing of the hydrophones. This could make localizing the source difficult, as we observed. The coastal array was placed along a cape in the St. Lawrence. This localization facilitated the deployment to rapidly access the sound channel. However, the proximity of the shore and cape wall gave rise to strong reflections and multipaths, which can sometimes hinder precise detection of the TDoAs. The St. Lawrence AURALS M1 were placed in the sound channel to maximize the reception range. Some

instruments were however moored on the southern border of the deep channel, which unfortunately placed them within the St. Lawrence outflow (Saucier and Chassé 2000). They were therefore subject to flow noise, which often masked the calls. Both critical habitats considered here are high-energy environments with strong tidal forcing (e.g. Saucier and Chassé 2000). It is therefore inaccurate to assume a constant propagation medium in space and time. The changes of the characteristics of the propagation medium must therefore be incorporated in the localization process to minimize the error. This can be accomplished with repeated visits of a grid of stations for CTD profiling, or the use of a ground-truthed 3D tidal circulation model. Frequent checks of the performance of the localization algorithm with transmitted sounds from known locations are likely to be essential for accurate monitoring with passive acoustics. The deployment of fixed acoustic pingers regularly transmitting a sound in the study area during the observation period should help to monitor the localization performance and take into account the main components of its variability.

## 5. ACKNOWLEDGEMENTS

This work was supported by the Fisheries and Oceans Canada (DFO) Chair in applied marine acoustics at ISMER-UQAR, DFO Maurice Lamontagne Institute species at risk program, and Canada Economic Development. We thank: the crews of the M/V Coriolis II and NGCC Isle Rouge for the deployment and recovery of the hydrophone array and AURAL M1 moorings in the St. Lawrence; all DFO, ISMER and Multi-Electronics technicians, students and assistants involved in preparing the material, its deployment at sea and the data acquisition. We thank Parks Canada for the access to Cap-de-Bon-Désir facility in the Saguenay—St. Lawrence Marine Park, and B. Long, INRS-ETE, for making available the DGPS location of the seismic sparker echosounder. Finally we thank the organisers of the workshop who provided the Bay of Fundy data set.

## 6. REFERENCES

- Cato, D.H. 1998. Simple methods of estimating source levels and locations of marine animal sounds. *J. Acoust. Soc. Am.* 104: 1667-1678.
- Cummings, W.C., Holliday, D.V., 1985. Passive acoustic location of bowhead whales in a population census off Point Barrow, Alaska. *J. Acoust. Soc. Am.* 78: 1163-1169.
- Martin, R. 2001. Noise power spectral density estimation based on optimal smoothing and minimum statistics. *Speech and Audio Processing, IEEE Transactions* 9: 504-512.
- McDonald, M.A., and Fox, C.G. 1999. Passive acoustic methods applied to fin whale population density estimation. *J. Acoust. Soc. Am.* 15: 2643-2651.

- Saucier, F.J., and Chassé, J. 2000. Tidal circulation and buoyancy effects in the St. Lawrence estuary. *Atmosphere-Ocean* 38: 505-556.
- Simard, Y., Lavoie, D., and Saucier, F.J. 2002. From plankton to whales: Oceanography of a traditional whale feeding ground and marine park in the St. Lawrence estuary. *ICES CM* 2002/N:14.
- Spiesberger, J.L. 1999. Locating animals from their sounds and tomography of the atmosphere: Experimental demonstration. *J. Acoust. Soc. Am.* 106: 837-846.
- Spiesberger, J.L. 2001. Hyperbolic location errors due to insufficient numbers of receivers. *J. Acoust. Soc. Am.* 109: 3076-3079.
- Spiesberger, J.L., and Fristrup, K.M. 1990. Passive localization of calling animals and sensing of their acoustic environment using acoustic tomography. *Am. Nat.* 135: 107-153.
- Spiesberger, J.L., and Wahlberg, M. 2002. Probability density functions for hyperbolic and isodiachronic locations. *J. Acoust. Soc. Am.* 112: 3046-3052.
- Tiemann, C.O., Porter, M.B., and Fraser, L.N. 2001. Automated model-based localization of marine mammals near Hawaii. In *Conference Proceedings of Oceans 2001 MTS/IEEE*, pp.1395-1400.
- Tiemann, C.O., and Porter, M.B. 2003. A comparison of model-based and hyperbolic localization techniques as applied to marine mammal calls. *J. Acoust. Soc. Am.* 114: 2406.
- Wahlberg, M., Mohl, B., and Madsen P.T. 2001. Estimating source position accuracy of a large-aperture hydrophone array for bioacoustics. *J. Acoust. Soc. Am.* 109: 397-406.
- Watkins, W. A., and Schevill, W.E. 1972. Sound source location by arrival-times on a non-rigid three-dimensional hydrophone array. *Deep-Sea Res.* 19: 691-706.
- Watkins, W.A., Daher, M.A., Reppucci, G.M., George, J.E., Martin, D.L., DiMarzio, N.A., and Gannon, D.P. 2000. Seasonality and distribution of whale calls in the North Pacific. *Oceanography* 13: 62-67.
- 

